Available online at http://scik.org
Commun. Math. Biol. Neurosci. 2022, 2022:30
https://doi.org/10.28919/cmbn/7122
ISSN: 2052-2541

A NOTE ON FRACTIONAL-ORDER MODEL FOR CHOLERA DISEASE TRANSMISSION WITH CONTROL STRATEGIES

MLYASHIMBI HELIKUMI[1,*], PARIDE O. LOLIKA[2]

[1]Mbeya University of Science and Technology, Department of Mathematics and Statistics, College of Science and Technical Education, P.O. Box 131, Mbeya, Tanzania

[2]University of Juba, Department of Mathematics, P.O. Box 82 Juba, Central Equatoria, South Sudan

Abstract. In this paper, we formulated and analyzed a fractional-order model for cholera disease transmission that consists of human population and surrounding environment. Three control strategies namely: health education campaigns, hygiene practices, and treatment of infected individuals are investigated. We divided the human population into three sub-classes namely: Susceptible, infected and recovered classes. The main assumptions on the disease transmission were that susceptible humans acquire the disease through contact with either infected humans or directly from environment. Mathematical analysis of the model was carried out and the threshold quantity R_0 which determine the existence of the disease in the population was determined. The model analysis showed that the disease exist in the population whenever $R_0 > 1$ and dies wherever $R_0 \leq 1$. It was also noted that both the disease-free and endemic equilibria are globally stable. Further more, we performed the numerical simulations of the model and the results showed that the order of derivatives have the influence on spread of cholera disease in the population. It was also noted that both the aforementioned control strategies have the potential to minimize the spread of cholera in the community.

Keywords: vibrio cholerae; model formulation; fractional order derivatives; model equilibria.

2010 AMS Subject Classification: 34K37, 93A30.

*Corresponding author

E-mail address: mhelikumi@yahoo.co.uk

Received December 29, 2021

1. INTRODUCTION

Cholera is an infectious intestinal disease caused by the bacterial species Vibrio cholerae [13]. Infectious bacterial cells are carried in vomits or faeces of infected people and spread in the population through the fecal-oral route [14]. The disease is manifested by severe diarrhea and excessive vomiting when a person ingests contaminated water or food [15]. The disease has for years been a major source of public health concern and an indication of the inadequacy of social amenities in developing countries. The recent cholera outbreaks in Zimbabwe [16], Yemen [17], Ethiopia [18], Kenya [19], Tanzania [20] and other countries continue to put the disease in the global limelight. The transmission dynamics of cholera involve several interactions of humans, pathogens, and the environment [21], which form direct human-to-human and indirect environment-to-human transmission pathways. Owing to its huge impact on economic development and public health, cholera has extensively been researched experimentally, clinically, and theoretically. Eradication of cholera is possible with appropriate measures such as hygienic practices, and treatment of infected individuals. Cognizant of this, efforts have been made to develop feasible intervention and prevention strategies for many years.

Mathematical models to study the dynamics and controls of infectious diseases have been formulated and studied by many mathematicians (see, [38, 23, 7, 24, 36]). Among the efforts which have been made to comprehend the complex dynamics of cholera disease transmissions [22]. In [31], a mathematical model of cholera epidemic with optimal control strategies using Pontryagin's maximum principle was formulated and studied. The study considered vaccination, treatment, and awareness programs as the control measures to the spread of cholera disease in the population. However, the model did not include the provision of safe domestic water as one of the control parameters. Authors in [26], proposed a model to study the cholera outbreak in Zimbabwe between 2008 and 2009. The model included both direct (human-to-human) and indirect (environment-to-human) transmission pathways and established the significance of the human-to-human transmission pathway in African cholera epidemics. Study in [27] modified the cholera model proposed and studied in [28], added more control options, and analyzed the optimal intervention strategies, but no human-to-human infection route was considered. [29]

proposed and analyzed a deterministic cholera model in Tanzania and incorporated human educational campaigns and water treatment as the control strategies. Nevertheless, in their model analysis, the basic reproduction number which is a threshold value for disease dynamics was not quantitatively analyzed. Authors in [25] also proposed a mathematical model on the control of cholera based on hygiene practices as a control strategy. However, their model did not incorporate the provision of safe domestic water as one of the control strategies. Other recent cholera models include those in [30], [35], [32], [34], and [33], highlighted that cholera can be controlled using suitable preventive strategies. However, most of these models did not incorporate human awareness campaigns, hygiene practices coupled with treatment of infected individuals as part of control strategies.

In recent years, researchers have been working on developing mathematical models using fractional-order derivatives. Many researchers have proposed different types of fractional and non-local derivatives, suggesting a decrease in all order derivatives, see [37, 38, 39]. For example, Riemann-Liouville introduced fractional-order differential theory which was further modified by Caputo [53, 40]. Both Rie-mann-Liouville and Caputo operators are called fractional derivatives with singular kernels [41]. Modeling physical problems using fractional-order derivatives received many attentions in both biological and engineering systems see, [42, 43, 44, 45, 46, 47, 48]. This is because fractional-order operators enlarge the region of stability, capture the memory dynamics and genetic properties which exist in both biological and engineering systems [49]. It is well known that integer order derivatives do not capture memory effects and are convenient for the local systems without the effect of external forces [50]. In addition, fractional-order derivatives can provide a better fit for real data for different disease models see, [51, 52, 53]. These are the advantages of modeling physical problems using fractional operators that are not included in integer-order derivatives.

Therefore, motivated by the above studies on fractional-order derivatives, we proposed and analyzed a fractional-order model of cholera disease transmission that incorporates the effect of human awareness campaign, hygiene practice and treatment of infected individuals. The paper is organized in the following form: In section 2 we present the model formulation; section

3 we perform the model analysis of the proposed model; followed by model simulations and discussions in section 4, and finally conclusion remarks is presented in section 5.

2. MODEL FORMULATION

In this section, the Caputo fractional-order derivative has been used to define the model differential equations for cholera disease transmission. The compartments proposed in this study are used to represent the epidemiological status of each human population and the concentration of *Vibrio bacteria* in the environment. The proposed and studied model is governed by the following assumptions:

(i) We sub-divided compartments for the humans into three sub-classes: susceptible $S(t)$, infectious $I(t)$, and recovered $R(t)$ populations. Thus, the total population of human is denoted by $N(t)$, defined by: $N(t) = S(t) + I(t) + R(t)$. The *Vibrios* concentration in the environment is denoted by $B(t)$, and the parameter K, denotes the half saturation concentration of *Vibrios* in the environment

(ii) Throughout the document, variables and parameters are assumed to be no-negative and are defined as follows: Λ and μ represent the rate of new recruitment and natural mortality rate of human populations respectively; $\frac{1}{\alpha}$ represents the average time in which humans spend in the infectious period.

(iii) We are assumed that humans become aware of the disease from education campaigns and join the recovered class at the rate, θ and never loose their awareness and immunity in the same cholera outbreak. Infected individuals that fail to receive successful treatment succumb to the disease at the rate d and upon successful therapeutic treatment recover from the disease after an average of $\frac{1}{\alpha}$ days.

(iv) In addition, the parameter ω_1 denotes the rate of treatment of infected humans, ω_2 is the excise of hygiene practices to reduce the concentration of vibrio bacteria in the environment. Parameters β_h and β_e are the forces of infections between human-to-human and environment-to-human transmission respectively, and σ denotes the rate of human shedding vibrio bacteria in the environment.

Our assumptions on the dynamics of cholera disease in this document illustrated in figure 1 and corresponding model differential equations presented below:

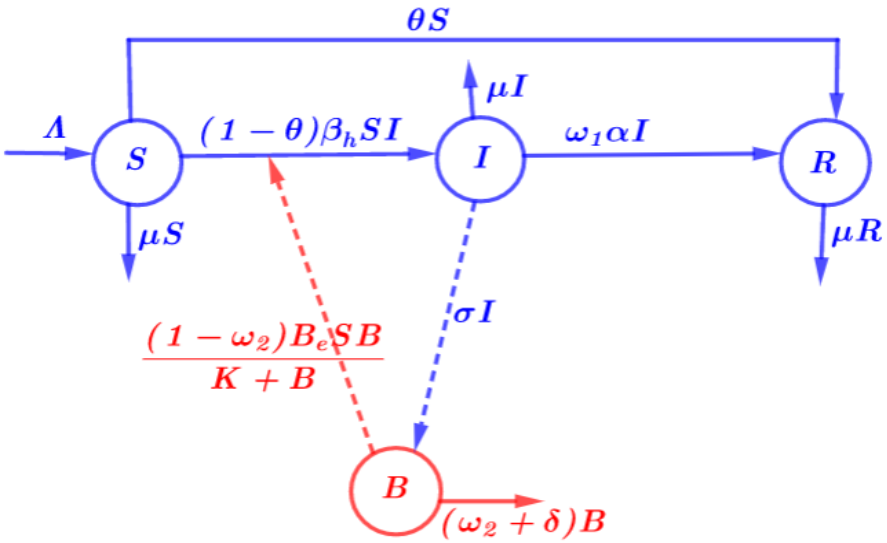

FIGURE 1. Flow chart for Cholera disease transmission

2.1. Model differential equations.

$$
(1)\quad \begin{cases}
{}_b^cD_t^q S(t) &= \Lambda^q - (1-\theta^q)\beta_h^q S(t)I(t) - (1-\omega_2^q)\beta_e^q \dfrac{S(t)B(t)}{k^q + B(t)} - (\mu^q + \theta^q)S(t), \\
{}_b^cD_t^q I(t) &= (1-\theta^q)\beta_h^q S(t)I(t) - (1-\omega_2^q)\beta_e^q \dfrac{S(t)B(t)}{k^q + B(t)} - (\mu^q + d^q + \omega_1^q\alpha^q)I(t), \\
{}_b^cD_t^q B(t) &= \sigma^q I(t) - (\omega_2^q + \delta^q)B(t), \\
{}_b^cD_t^q R(t) &= \omega_1^q\alpha^q I(t) + \theta^q S(t) - \mu^q R(t).
\end{cases}
$$

2.2. Preliminaries on the Caputo fractional calculus. We begin by introducing the definition of Caputo fractional derivative and state related theorems (see, [3, 4, 5, 41, 11]) that we will use to derive important results in this work.

Definition 1. *Suppose that $q > 0, t > b, q, b, t \in \mathbb{R}$, the Caputo fractional derivative is given by:*

$$
(2)\qquad {}_b^cD_t^q f(t) = \frac{1}{\Gamma(n-q)} \int_b^t \frac{f^n(\xi)}{(t-\xi)^{q+1-n}} d\xi, \quad n-1 < q, n \in \mathbb{N}.
$$

Definition 2. *(Caputo derivative of a constant* [41]*). The fractional derivative for a constant function $f(t) = c$ is zero, that is:*

$$ {}_b^c D_t^q c = 0. \tag{3}$$

Let us consider the following general type of fractional differential equations involving Caputo derivative:

$$ {}_b^c D_t^q x(t) = f(t, x(t)), \qquad q \in (0,1) \tag{4}$$

with initial condition $x_0 = x(t_0)$.

Definition 3. *(see* [3]*). The constant x^* is an equilibrium point of the Caputo fractional dynamic system (4) if and only if, $f(t, x^*) = 0$.*

In what follows, we present an extension of the Lyapunov direct method for Caputo type fractional order for nonlinear systems [3, 42].

Theorem 2.1. *(Uniform Asymptotic Stability* [3, 42]*). Let x^* be an equilibrium point for the non-autonomous fractional order system (4) and $\Omega \subset \mathbb{R}^n$ be a domain containing x^*. Let $L : [0,\infty) \times \Omega \to \mathbb{R}$ be a continuously differentiable function such that:*

$$M_1(x) \leq N(t, x(t)) \leq M_2(x)$$

and:

$$ {}_b^c D_t^q N(t, x(t)) \leq M_3(x),$$

for all $q \in (0,1)$ and all $x \in \Omega$, where $M_1(x)$, $M_2(x)$ and $M_3(x)$ are continuous positive definite functions on Ω. Then the equilibrium point of system (4) is uniformly asymptotically stable.

The following theorem summarizes a lemma proved in [3], where a Volterra-type Lyapunov function is obtained for fractional-order epidemic systems.

Lemma 1. *(see* [3]*. Let $x(\cdot)$ be a continuous and differentiable function with $x(t) \in \mathbb{R}_+$. Then, for any time instant $t \geq b$, one has:*

$$ {}_b^c D_t^q \left(x(t) - x^* - x^* \ln \frac{x(t)}{x^*} \right) \leq \left(1 - \frac{x^*}{x(t)} \right) {}_b^c D_t^q x(t), \qquad x^* \in \mathbb{R}^+, \qquad \forall q \in (0,1).$$

3. Model Analysis

3.1. Non-negativity and boundness of model system (1).

Theorem 3.1. *For the model system (1), there exists a unique solution in* $(0,\infty)$*, however, the solution is always positive for all values of* $t \geq 0$*and remains in* R^3_+.

Proof. From the model system (1), we first show that:

$R^3_+ = \{N(t) \in R^3_+ : N(t) \geq 0\}$ is positive invariant. Now we have to demonstrate that each hyper-plane bounding the positive orthant and the vector field points to R^3_+. Now consider the following: let us assume that there exists a $t_* > t_0$, such that $N(t_*) = 0$, and $N(t) < 0$ for $t \in (t_*, t_1)$, where t_1 is sufficiently close to t_*, if $N(t_*) = 0$ then we have that:

${}^c_b D^q_t N(t_*) - \Lambda^q > 0$. This implies that ${}^c_b D^q_t N(t) > 0$ for all $t \in [t_*, t_1]$. The above discussion shows that the three hyper-plane bounding the orthants, that is the vector field points to R^3_+. This shows that all the solutions of the model system (1) remains positive for all $t \geq 0$. □

Theorem 3.2. *Let* $\Phi(t) = N(t)$ *be the unique solution of the model system (1) for all* $t \geq 0$*, then the solution* $\Phi(t)$ *is bounded above, that is,* $\Phi(t) \in \Omega$ *where* Ω *is the feasible region defined as:*

$$\Omega = \left\{N(t) \in \mathbb{R}^3_+ 0 \leq N(t) \leq C_N.\right\}$$

which is interior denoted by $int(\Omega)$ *and given by:*

$$int(\Omega) = \left\{N(t) \in \mathbb{R}^3_+ 0 \leq N(t) \leq C_N.\right\}$$

Proof. Here we prove that the solutions of model system (1) are bounded for all $t \geq 0$. Biologically, the lowest possible value of each state of the model system (1) is zero. Next, we determine the upper-bound of states. Based on this discussion, it is easy to show that the following condition holds for biological relevance of species. $0 \leq N(t) \leq C_N$ From this condition one gets:

$${}^c_b D^q_t N(t) \leq \Lambda^q - \mu^q N(t)$$

From the Laplace transformation condition, one gets:

$$S^q L[N(t)] - S^{q-1}N(0) \leq \frac{\Lambda^q}{S} - \mu^q L[N(t)]$$

Collecting the terms, we have:

$$\begin{aligned} L[N(t)] &\leq \Lambda^q \frac{S^{-1}}{S^q+\mu^q} + N(0)\frac{S^{q-1}}{S^q+\mu^q}. \\ &= \Lambda^q \frac{S^{q-(1+q)}}{S^q+\mu^q} + N(0)\frac{S^{q-1}}{S^q+\mu^q} \end{aligned}$$

Using the inverse Laplace transform, we have:

$$\begin{aligned} N(t) &\leq L^{-1}\left\{p^q\Lambda^q \frac{S^{q-(1+q)}}{S^q+\mu^q}\right\} - N(0)L^{-1}\left\{\frac{S^{q-1}}{S^q+\mu^q}\right\} \\ &\leq \Lambda^q t^q E_{q,q+1}(-\mu^q)t^q + N(0)E_{q,1}(-\mu^q)t^q \\ &\leq \frac{\Lambda^q}{\mu^q} t^q E_{q,q+1}(-\mu^q)t^q + N(0)E_{q,1}(-\mu^q)t^q \\ &\leq Max\left\{\frac{\Lambda^q}{\mu^q}, N(0)\right\}\left(t^q E_{q,q+1}(-\mu^q)t^q + E_{q,1}(-\mu^q)t^q\right) \\ &= \frac{C}{\Gamma(1)} = C_N. \end{aligned}$$

Where $C_N = Max\left\{\frac{\Lambda^q}{\mu^q}, N(0)\right\}$. Therefore, $N(t)$ is bounded above and this complete the proof. □

3.2. Model Equilibria and Stability Analysis.

3.2.1. *Disease-free equilibrium and the basic reproduction number.* Since $R(t)$ does not appear in all the equations in system (1), it is sufficient to analyze the solutions of system (5) for the behavior of the model differential equations (1).

$$(5) \quad \begin{cases} {}_b^c D_t^q S(t) &= \Lambda^q - (1-\theta^q)\beta_h^q S(t)I(t) - (1-\omega_2^q)\beta_e^q \dfrac{S(t)B(t)}{k^q+B(t)} - (\mu^q+\theta^q)S(t), \\ {}_b^c D_t^q I(t) &= (1-\theta^q)\beta_h^q S(t)I(t) - (1-\omega_2^q)\beta_e^q \dfrac{S(t)B(t)}{k^q+B(t)} - (\mu^q+d^q+\omega_1^q\alpha^q)I(t), \\ {}_b^c D_t^q B(t) &= \sigma^q I(t) - (\omega_2^q+\delta^q)B(t). \end{cases}$$

In what follows, we compute the threshold quantity R_0 which determines the power of a disease to spread in the population. The model system (5) always has a disease-free equilibrium E^0

given by:

$$E^0 : \left(S^0, I^0, B^0\right) = \left(\frac{\Lambda^q}{\mu^q + \theta^q}, 0, 0\right).$$

Following the next generation matrix approach as used in [6, 2],the non-negative matrix F that denotes the generation of new infection and the non-singular matrix V that denotes the disease transfer among compartments evaluated at E^0 are defined as follows;

$$F = \begin{pmatrix} \frac{(1-\theta^q)\beta_h^q \Lambda^q}{(\mu^q + \theta^q)} & \frac{(1-\omega_2^q)\beta_e^q \Lambda^q}{k(\mu^q + \theta^q)} \\ 0 & 0 \end{pmatrix} \tag{6}$$

$$V = \begin{pmatrix} (\mu^q + d^q + \omega_1^q \alpha^q) & 0 \\ -\sigma^q & (\omega_2^q + \delta^q) \end{pmatrix} \tag{7}$$

Therefore, from equations (6) and (7), it can easily be verified that the basic reproduction number R_0 of system (1) is:

$$R_0 \quad = \quad R_{0h} + R_{0e} \tag{8}$$

Where by:

$$R_{0e} = \frac{(1-\omega_2^q)\sigma^q \beta_e^q}{k^q(\mu^q + \theta^q)(\omega_2^q + \delta^q)} \tag{9}$$

$$R_{0h} = \frac{(1-\theta^q)\Lambda^q \beta_h^q}{(\mu^q + \theta^q)(\mu^q + d^q + \omega_1^q \alpha^q)} \tag{10}$$

The basic reproduction number R_0 is defined as the expected number of secondary cases of human infections produced in a completely susceptible population by one infected individual during its lifetime as infectious. The terms R_{0e} and R_{0h} refer to the human-to-human and environment-to-human disease transmissions respectively.

3.2.2. *Stability of the model equilibria.* Our goal in this section is to investigate the stability of the disease-free and endemic equilibria of the model system (5).

Theorem 3.3. *if $R_0 < 1$ the disease-free equilibrium point (DFE) of the system (1) is locally asymptotically stabe when $R_0 < 1$ and unstable if $R_0 > 1$.*

Proof. To prove the theorem (3.3), we evaluate the Jacobean matrix of system (5) at the disease-free equilibrium and investigate the behavior of eigenvalues. In what follows the Jacobean matrix of the system (5) evaluated at the disease-free equilibrium is given by:

(11)
$$J_{DFE} = \begin{pmatrix} -(\theta^q+\mu^q) & -(1-\omega_3^q)\dfrac{\beta_h^q\Lambda^q}{(\theta^q+\mu^q)} & -(1-\omega_2^q)\dfrac{\beta_e^q\Lambda^q}{k^q(\theta^q+\mu^q)} \\ 0 & (1-\theta^q)\frac{\beta_h^q\Lambda^q}{(\theta^q+\mu^q)}-(\mu^q+d^q+\omega_1^q\alpha^q) & (1-\omega_2^q)\frac{\beta_e^q\Lambda^q}{k^q(\theta^q+\mu^q)} \\ 0 & \sigma^q & -(\omega_2^q+\delta^q) \end{pmatrix}$$

The first eigenvalue of matrix (11) is given by $\lambda_1 = -(\theta^q+\mu^q)$ which is non-positive. The remaining two eigenvalues are obtained in the following matrix:

(12)
$$M = \begin{pmatrix} (1-\theta^q)\dfrac{\beta_h^q\Lambda^q}{(\theta^q+\mu^q)}-(\mu^q+d^q+\omega_1^q\alpha^q) & (1-\omega_2^q)\dfrac{\beta_e^q\Lambda^q}{k^q(\theta^q+\mu^q)} \\ \sigma^q & -(\omega_2+\delta^q) \end{pmatrix}$$

It follows that, we find the characteristic polynomial of the matrix (12) which is given as follows:

(13)
$$\lambda^2+\left[-(\mu^q+d^q+\omega_1^q\alpha^q)(R_{0h}-1)+(\omega_2^q+\delta^q)\right]\lambda-(\omega_2^q+\delta^q)\left[(\mu^q+d^q+\omega_1^q\alpha^q)(R_{0h}-1)+R_{0e}\right]=0$$

Since the coefficients of the characteristic polynomial (13) are all non-negative for $R_{0h}<1$ and $R_{0e}<1$, then we conclude that for $R_0<1$ the disease-free equilibrium E^0 of the system (1) is locally asymptotically stable and this completes the proof. □

Theorem 3.4. *The disease-free equilibrium E^0 is globally asymptotically stable if $R_0 \leq 1$, otherwise is unstable.*

Proof. To prove the theorem (3.4), we first evaluate the model system (5) at the point E^0 which leads to the following system:

(14)
$$\begin{cases} {}_b^cD_t^qS(t) &= S(t)\left(\Lambda^q(\dfrac{1}{S(t)}-\dfrac{1}{S^0})-(1-\theta^q)\beta_h^qI(t)-(1-\omega_2^q)\dfrac{\beta_e^qB(t)}{k^q+B(t)}\right), \\ {}_b^cD_t^qI(t) &= \left((1-\theta^q)\beta_h^qI(t)+(1-\omega_2^q)\dfrac{\beta_e^qB(t)}{k^q+B(t)}\right)\left(S^0+(S(t)-S^0)-(\mu^q+d^q+\omega_1^q+\alpha^q)\right), \\ {}_b^cD_t^qB(t) &= \sigma^qI(t)-(\omega_2^q+\delta^q)B(t). \end{cases}$$

In what follows, we consider the following Lyapunov functional:

$$L_0(t) = \left\{ S(t) - S^0 - S^0 \ln \frac{S(t)}{S^0} \right\} + I(t) + \frac{\mu^q + d^q + \omega_1^q \alpha^q}{\sigma^q} B(t). \tag{15}$$

Taking the derivative of $L(t)$ along the system (14) and making simplifications, one gets:

$$\begin{aligned} {}_b^c D_t^\theta L_0(t) &\leq \Lambda^q \left(2 - \frac{S(t)}{S^0} - \frac{S^0}{S(t)} \right) + \left(\mu^q + d^q + \omega_1^q \alpha^q \right) \left(R_{0h} - 1 \right) I(t) \\ &\quad + \left(\omega_2^q + \delta^q \right) \left(R_{0e} - 1 \right) B(t). \end{aligned} \tag{16}$$

Since all the parameters and variables in system (16) are non-negative, it follows that ${}_b^c D_t^\theta L_0(t) < 0$ holds if $\mathscr{R}_{0h} < 1$ and $\mathscr{R}_{0e} < 1$. Moreover, ${}_b^c D_t^\theta L_0(t) = 0$ if and only if $S(t) = 0$, $I(t) = 0$, $B(t) = 0$, for all $t \geq 0$. Thus, $\mathscr{L}_0(t)$ is Lyapunov function on Ω. Using Lasalle Invariance principle [1], it implies that every solution of the system (5) approaches the disease-free equilibrium point E^0 as $t \to \infty$. Therefore, we conclude that the disease-free equilibrium point of system (5) is globally asymptotically stable whenever $R_0 \leq 1$. This completes the proof. □

Theorem 3.5. *The Model system (5) has endemic equilibrium point E^* which is globally asymptotically stable for $R_0 > 1$.*

Proof. To prove the theorem (3.5), we consider the following Lyapunov functional:

$$L_0(t) = C_1 \left\{ S(t) - S^* - S^* \ln \frac{S(t)}{S^*} \right\} + C_2 \left\{ I(t) - I^* - I^* \ln \frac{I(t)}{I^0} \right\} + C_3 \left\{ B(t) - B^* - B^* \ln \frac{B(t)}{B^*} \right\}. \tag{17}$$

Differentiating $L_1(t)$ one gets the following:

$${}_b^c D_t^q L_1(t) \leq C_1 \left(1 - \frac{S^*}{S} \right) {}_b^c D_t^q S(t) + C_2 \left(1 - \frac{I^*}{I(t)} \right) {}_b^c D_t^q I(t) + C_3 \left(1 - \frac{B^*}{B(t)} \right) {}_b^c D_t^q B(t). \tag{18}$$

In what follows, we substitute (1) in (18) and we get the following:

$$\begin{aligned} {}_b^c D_t^\theta L_1(t) &\leq C_1 \left(1 - \tfrac{S^*}{S(t)} \right) \left(\Lambda^q - (1-\theta^q)\beta_h^q S(t) I(t) - (1-\omega_2^q)\beta_e^q \frac{S(t)B(t)}{k^q + B(t)} - (\mu^q + \theta^q) S(t) \right) \\ &+ C_2 \left(1 - \tfrac{V^*}{V(t)} \right) \left((1-\theta^q)\beta_h^q S(t) I(t) - (1-\omega_2^q)\beta_e^q \frac{S(t)B(t)}{k^q + B(t)} - (\mu^q + d^q + \omega_1^q \alpha^q) I(t) \right) \\ &+ C_3 \left(1 - \tfrac{B^*}{B(t)} \right) \left(\sigma^q I(t) - (\omega_2^q + \delta^q) B(t) \right). \end{aligned} \tag{19}$$

Let us set the system (5) at the endemic equilibrium point, that is:

$$
(20)\quad \begin{cases} \mu^q+\theta^q &= \dfrac{\Lambda^q}{S^*}-(1-\theta^q)\beta_h^q I^*-(1-\omega_2^q)\dfrac{\beta_e^q B^*}{k^q+B^*} \\ (\mu^q+d^q+\omega_1^q\alpha^q) &= (1-\theta^q)\beta_h^q S^*+(1-\omega_2^q)\beta_e^q\dfrac{S^*B^*}{I^*(k^q+B^*)}, \\ f^{(\omega_2^q+\delta^q)} &= \dfrac{\sigma^q I^*}{B^*}, \\ f^*(B) &= \dfrac{B^*}{k^q+B^*}. \end{cases}
$$

By substituting (20) in (19) and setting the constants $B_i=1$ with $i=1,2,3$, one gets the following after simplifications:

$$
(21)\quad \begin{cases} {}_b^cD_t^\theta L_1(t) &\leq \dfrac{\Lambda^q}{S^*}\left(2-\dfrac{S(t)}{S^*}-\dfrac{S^*}{S(t)}\right)+(1-\theta^q)\beta_h^q I^*\left(\dfrac{S(t)}{S^*}-\dfrac{S(t)I(t)}{S^*I^*}+\dfrac{I(t)}{I^*}-1\right) \\ &\quad +(1-\omega_2^q)\beta_e^q f^*(B)\left(\dfrac{S(t)}{S^*}+\dfrac{S^*}{S(t)}\dfrac{I^*}{I(t)}-\dfrac{I(t)}{I^*}+1\right) \\ &\quad +(1-\theta^q)\beta_h^q S^*\left(1-\dfrac{S(t)}{S^*}-\dfrac{I(t)}{I^*}+\dfrac{I(t)S(t)}{I^*S^*}\right) \\ &\quad +(1-\omega_2^q)\beta_e^q\dfrac{f^*(B)S^*}{I^*}\left(\dfrac{f(B)}{f^*(B)}-\dfrac{f(B)I^*}{f^*(B)I(t)}-\dfrac{I(t)}{I^*}+1\right) \end{cases}
$$

Note that $x-1\geq \ln(x)$ for any $x>0$, and this holds if and only if $x=1$. In what follows, we have:

$$
(22)\quad \begin{cases} \left(\dfrac{S(t)}{S^*}-\dfrac{S(t)I(t)}{S^*I^*}+\dfrac{I(t)}{I^*}-1\right) &= \leq \ln\dfrac{S(t)}{S^*}-\dfrac{S(t)}{S^*}+\ln\dfrac{S(t)I(t)}{S^*I^*}+\dfrac{I(t)}{I^*}-\ln\dfrac{I(t)}{I^*} \\ &\quad = \ln\dfrac{S(t)}{S^*}-\dfrac{S(t)}{S^*}+\dfrac{I(t)}{I^*}-\ln\dfrac{I(t)}{I^*} \\ \left(\dfrac{S(t)}{S^*}+\dfrac{S^*}{S(t)}\dfrac{I^*}{I(t)}-\dfrac{I(t)}{I^*}+1\right) &\leq \ln\dfrac{I(t)}{I^*}-\dfrac{I(t)}{I^*}+\dfrac{S^*I^*}{S(t)I(t)}-\ln\dfrac{I^*S^*}{I(t)S(t)} \\ \left(1-\dfrac{S(t)}{S^*}-\dfrac{I(t)}{I^*}+\dfrac{I(t)S(t)}{I^*S^*}\right) &\leq \ln\dfrac{S(t)}{S^*}-\dfrac{S(t)}{S^*}+\dfrac{I(t)S(t)}{I^*S^*}-\ln\dfrac{I(t)S(t)}{I^*S^*} \\ \left(\dfrac{f(B)}{f^*(B)}-\dfrac{f(B)I^*}{f^*(B)I(t)}-\dfrac{I(t)}{I^*}+1\right) &= \leq \ln\dfrac{f(B)I^*}{f^*(B)I(t)}+\dfrac{f(B)}{f^*(B)}-\ln\dfrac{f(B)}{f^*(B)}+\ln\dfrac{I(t)}{I^*}-\dfrac{I(t)}{I^*} \\ &\quad = \dfrac{f(B)}{f^*(B)}-\ln\dfrac{f(B)}{f^*(B)}+\ln\dfrac{I(t)}{I^*}-\dfrac{I(t)}{I^*} \end{cases}
$$

Since $\left(2-\frac{S(t)}{S^*}-\frac{S^*}{S(t)}\right)\leq 0$, it follows from equation (22) yields the following:

$$
(23)\quad \begin{cases} {}_b^cD_t^\theta L_1(t) &\leq +(1-\omega_3^q)\beta_h^q I^*\left(\ln\dfrac{S(t)}{S^*}-\dfrac{S(t)}{S^*}+\dfrac{I(t)}{I^*}-\ln\dfrac{I(t)}{I^*}\right) \\ &\quad +(1-\omega_2^q)\beta_e^q f^*(B)\left(\ln\dfrac{I(t)}{I^*}-\dfrac{I(t)}{I^*}+\dfrac{S^*I^*}{S(t)I(t)}-\ln\dfrac{I^*S^*}{I(t)S(t)}\right) \\ &\quad +(1-\omega_3^q)\beta_h^q S^*\left(\ln\dfrac{S(t)}{S^*}-\dfrac{S(t)}{S^*}+\dfrac{I(t)S(t)}{I^*S^*}-\ln\dfrac{I(t)S(t)}{I^*S^*}\right) \\ &\quad +(1-\omega_2^q)\beta_e^q\dfrac{f^*(B)S^*}{I^*}\left(\dfrac{f(B)}{f^*(B)}-\ln\dfrac{f(B)}{f^*(B)}+\ln\dfrac{I(t)}{I^*}-\dfrac{I(t)}{I^*}\right) \end{cases}
$$

Since the arithmetic mean is greater than or equal to the geometrical mean, it follows that; from (23), one can note that ${}_b^cD_t^qL_1(t) \leq 0$ whenever $R_0 > 1$. Therefore, using Lasalle Invariance principle [1], the system (1) has a global asymptotically stable equilibrium point for all $R_0 \geq 1$ and this completes the proof. □

4. NUMERICAL SIMULATIONS

In this section, we perform the numerical simulations of the model system (1) using MATLAB programming language to support the analytical results and determine the effects of proposed control strategies. We utilized the fractional Adam-Bashforth-Moulton scheme to simulate the model (1) as illustrated below;

Consider the nonlinear differential equation:

$$ {}_b^cD_t^q\Phi(t) = f(t,\Phi(t)), 0 \leq t \leq T \tag{24}$$

With the initial conditions:

$$ \Phi^p(t) = \Phi_0^p, \quad p = 0,1,2,...[q]-1 \tag{25}$$

Now, with operating by the fractional integral operator on the equation 24, we can obtain on the solution $\Phi(t)$ by solving the following equation:

$$ \Phi^p(t) = \sum_{p=0}^{|q|-1} \frac{\Phi^p}{p!}t^p + \frac{1}{\Gamma(q)}\int_0^t (t-\tau)^{q-1} f(\tau,\Phi(\tau))d\tau \tag{26}$$

Diethelm [5] used the predictor-corrector scheme based on the Adam-Bashforth-Moulton algorithm to solve the equation 24. setting $h = \frac{T}{N}$, $t_n = nh$and $n = 0,1,2,...,N \in Z^+$. Therefore we can discrete the equation 26 as follows:

$$ \Phi_h(t_{n+1}) = \sum_{p=0}^{|q|-1} \frac{\Phi_0^p}{p!}t_{n+1}^p + \frac{h^q}{\Gamma(q+2)}\sum_{m=0}^{n} a_{m,n+1} f(t_m,\Phi_m) + \frac{h^q}{\Gamma(q+2)} f(t_{n+1},\Phi_{n+1}^v) \tag{27}$$

where by $t_m = mh$ with some fixed h and:

$$ a_{m,n+1} = \begin{cases} n^{q+1} - (n-q)(n+q)^q, & m = 0, \\ (n-m+2)^{q+1} + (n-m)^{q+1} - 2(n-m+1)^{q+1}, & 1 \leq m \leq n, \\ 1 & if \quad m = n+1. \end{cases}$$

and the predicted value :

$$\Phi^p_{t_n+1} = \sum_{p=0}^{|q|-1} \frac{\Phi_0^p}{p!} t_{n+1}^p + \frac{1}{\Gamma(q)} \sum_{m=0}^{n} b_{m,n+1} f(t_m, \Phi_h(t_m)) \tag{28}$$

With

$$b_{m,n+1} = \frac{h^q}{q}\Big((n+1-m)^q - (n-m)^q\Big) \tag{29}$$

The error estimate is

$$\max_{0\le m\le k} |\Phi(t_m) - \Phi_h(t_m)| = O(h^p) \tag{30}$$

with $k \in N$ and $p = \min(2, n+q)$

4.1. Application of Adam-Bashforth-Moulton Scheme to the proposed model. In this section, we utilize the Adam-Bashforth-Moulton method to numerically solve the nonlinear fractional model (1). In the view to the generalized Adam-Bashforth-Moulton scheme, the proposed model (1) has the following form:

$$\begin{cases}
S(t_{n+1}) &= S_0 + \dfrac{h^q}{\Gamma(q+2)} f_S\big(t_{n+1}, S^p(t_{n+1}), I^p(t_{n+1}), R^p(t_{n+1}), B^p(t_{n+1})\big) \\
&\quad + \dfrac{h^q}{\Gamma(q+2)} \displaystyle\sum_{m=0}^{n} a_{m,n+1} f_S\big(t_m, S(t_m), I(t_m), R(t_m), B(t_m)\big), \\
I(t_{n+1}) &= I_0 + \dfrac{h^q}{\Gamma(q+2)} f_I\big(t_{n+1}, S^p(t_{n+1}), I^p(t_{n+1}), R^p(t_{n+1}), B^p(t_{n+1})\big) \\
&\quad + \dfrac{h^q}{\Gamma(q+2)} \displaystyle\sum_{m=0}^{n} a_{m,n+1} f_I\big(t_m, S(t_m), I(t_m), R(t_m), B(t_m)\big), \\
R(t_{n+1}) &= R_0 + \dfrac{h^q}{\Gamma(q+2)} f_R\big(t_{n+1}, S^p(t_{n+1}), I^p(t_{n+1}), R^p(t_{n+1}), B^p(t_{n+1})\big) \\
&\quad + \dfrac{h^q}{\Gamma(q+2)} \displaystyle\sum_{m=0}^{n} a_{m,n+1} f_R\big(t_m, S(t_m), I(t_m), R(t_m), B(t_m)\big), \\
B(t_{n+1}) &= B_0 + \dfrac{h^q}{\Gamma(q+2)} f_B\big(t_{n+1}, S^p(t_{n+1}), I^p(t_{n+1}), R^p(t_{n+1}), B^p(t_{n+1})\big) \\
&\quad + \dfrac{h^q}{\Gamma(q+2)} \displaystyle\sum_{m=0}^{n} a_{m,n+1} f_B\big(t_m, S(t_m), I(t_m), R(t_m), B(t_m)\big).
\end{cases} \tag{31}$$

Where:

$$
(32)\qquad \begin{cases} S^p(t_{n+1}) &= S_0+\dfrac{1}{\Gamma q}\displaystyle\sum_{m=0}^{n} b_{m,n+1} f_S(t_m,S(t_m),I(t_m),R_(t_m),B(t_m)),\\ I^p(t_{n+1}) &= I_0+\dfrac{1}{\Gamma q}\displaystyle\sum_{m=0}^{n} b_{m,n+1} f_I(t_m,S(t_m),I(t_m),R_(t_m),B(t_m)),\\ R^p(t_{n+1}) &= R_0+\dfrac{1}{\Gamma q}\displaystyle\sum_{m=0}^{n} b_{m,n+1} f_R(t_m,S(t_m),I(t_m),R_(t_m),B(t_m)),\\ B^p(t_{n+1}) &= B_0+\dfrac{1}{\Gamma q}\displaystyle\sum_{m=0}^{n} b_{m,n+1} f_B(t_m,S(t_m),I(t_m),R_(t_m),B(t_m)). \end{cases}
$$

In what follows we have:

$$
(33)\begin{cases} f_S(t_m,S(t_m),I(t_m),R(t_m),B(t_m)) &= \Lambda^q-(1-\omega_3^q)\beta_h^q S(t)I(t)-(1-\omega_2^q)\beta_e^q\dfrac{S(t)B(t)}{k^q+B(t)}\\ &\quad -(\mu^q+\theta^q)S(t),\\ f_I(t_m,S(t_m),I(t_m),R(t_m),B(t_m)) &= (1-\omega_3^q)\beta_h^q S(t)I(t)-(1-\omega_2^q)\beta_e^q\dfrac{S(t)B(t)}{k^q+B(t)}\\ &\quad -(\mu^q+d^q+\omega_1^q\alpha^q)I(t),\\ f_R(t_m,S(t_m),I(t_m),R(t_m),B(t_m)) &= \sigma^q I(t)-(\omega_2^q+\delta^q)B(t),\\ f_B(t_m,S(t_m),I(t_m),R(t_m),B(t_m)) &= \omega_1^q\alpha^q I(t)+\theta^q S(t)-\mu^q R(t). \end{cases}
$$

Additionally, the quantities

$$
(34)\qquad \begin{cases} f_S(t_{n+1},S^p(t_{n+1}),I^p(t_{n+1}),R^p(t_{n+1}),B^p(t_{n+1})),\\ f_I(t_{n+1},S^p(t_{n+1}),I^p(t_{n+1}),R^p(t_{n+1}),B^p(t_{n+1})),\\ f_R(t_{n+1},S^p(t_{n+1}),I^p(t_{n+1}),R^p(t_{n+1}),B^p(t_{n+1})),\\ f_B(t_{n+1},S^p(t_{n+1}),I^p(t_{n+1}),R^p(t_{n+1}),B^p(t_{n+1})). \end{cases}
$$

are the derivatives from (33) at the point $t_{n+1}, n = 1,2,3,...m$.

In simulating the model system (1), we assumed the initial condition that $S(0) = 12, \quad I(0) = 1,$ and $B(0) = 230$. The parameters used in the model simulations are in table (1).

TABLE 1. Description of parameters used in the model system (1)

Symbol	Description	Value	Units	
Λ	New recruitment rate of humans	0.0000548	Years^{-1}	[9]
μ	Natural mortality rate of humans	0.02	Years^{-1}	[12]
β_e	environment-to-human transmission rate	0.124	Day^{-1}	[9]
β_h	Human-to-human transmission rate	0.0444	Day^{-1}	[9]
d	Disease mortality rate of humans	0.013	Day^{-1}	[10]
K	*Vibrio cholerae* concetration in the Environment	500	cells/ml	[12]
σ	Shedding rate of humans in the environment	10	cells/ml day^{-1}person^{-1}	[12]
δ	*Vibrio cholerae* decay in the environment	$\frac{1}{30}$	Day^{-1}	[12]
α	Recovery rate of infected humans	0.2	Day^{-1}	[12]
θ	Human awareness rate	Variable	Dimensionaless	
ω_1	Rate of teatment of infected humans	Variable	Dimensionaless	
ω_2	Effect of hygiene practices	Variable	Dimensionaless	

4.2. Sensitivity analysis of the reproduction number. The results from model system (1) have shown that the basic reproduction number is an important threshold parameter for persistence and extinction of cholera disease in the population. Most of the parameters in this study have been drawn from the literature and some were estimated, therefore, it is important. to perform the sensitivity analysis to demonstrate the influence of each parameter in the magnitude of basic reproduction number R_0.

Definition 4. *(See,* [8]*) The normalized sensitivity index of R_0 which depends on differentiably of parameter, ζ is defined as* $\Phi_{\zeta}^{R_0} = \frac{\partial R_0}{\partial \zeta} \times \frac{\zeta}{R_0}$.

The implication of the sensitivity analysis is that the model parameters whose sensitivity index is positive increase the magnitude of R_0 whenever they are increased and those with a negative index decrease the magnitude of R_0 whenever they are increased. Therefore, the value of normalized sensitivity index for each parameter used in the model (1) is summarized in table (2):

TABLE 2. Sensitivity analysis of parameters for the model system (1)

Parameter	Λ	μ	β_e	β_h	d	K	δ
Index	+0.0085	-0.0548	+0.4915	+0.0085	-0.0031	-0.4915	-0.0259
Parameter	σ	α	ω_1	ω_2	ω_3	θ	
Index	+0.4915	-0.0005	-0.0005	-1.2030	-0.0042	-0.45	

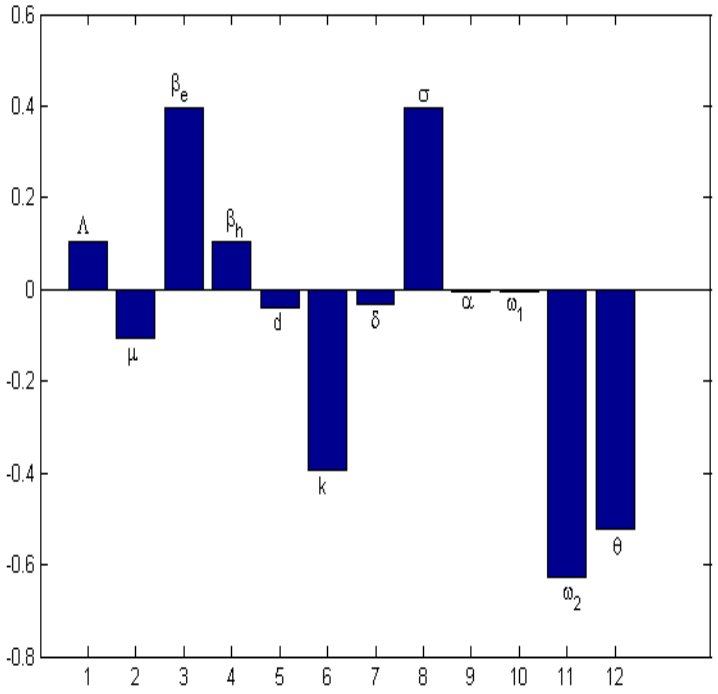

FIGURE 2. Sensitivity analysis of the model system (1)

From the results in Fig. 2, it was noted that model parameters Λ, β_e, β_h, and σ have a positive influence on the magnitude of R_0, that is, whenever they are increased, the magnitude of R_0 increases. For instance, an increase in β_e by 10% will lead to an increase in the magnitude of the magnitude of R_0 by 4.915%. Model parameters with negative index values have a negative influence on R_0, for example, an increase in ω_2 by 10% will lead to a decrease on R_0 by 12.030%.

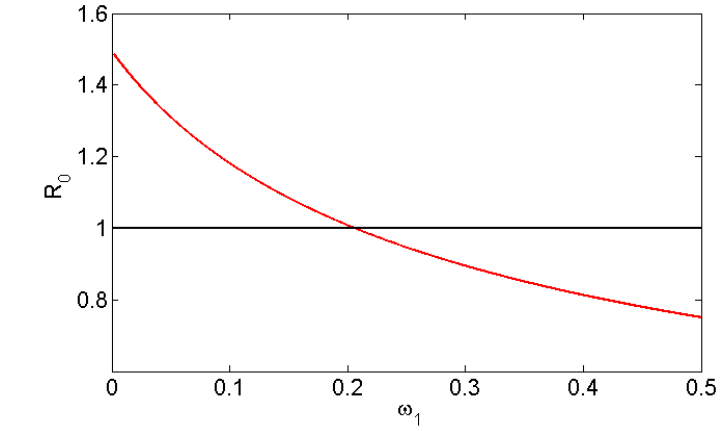

(a)

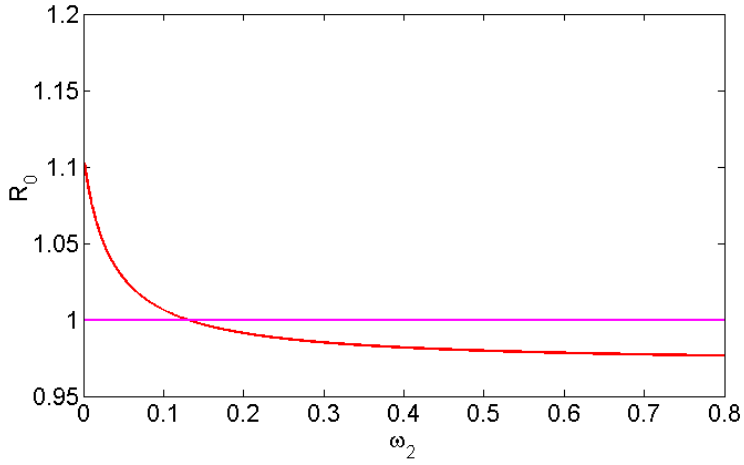

(b)

FIGURE 3. Effects of varying (a) Rate of treatment of infected humans ω_1 on R_0 (b) hygiene practices ω_2 on R_0

Numerical results in Fig. 3 (a), shows the effects of varying treatment rate ω_1 on R_0. From the results we noted that increasing the treatment rate of infected human (modeled by parameter ω_1) decreases the size of R_0. we can note that, whenever ω_1 is greater than 0.2 the disease dies in the community. In Figure 3 (b), we investigate the effect of hygiene practice, ω_2 on the spread of disease in the community. We noted that whenever the hygiene practive rate, ω_2 is greater than 0.1 the disease dies in the community which implies that exercising by 10% of hygiene practices, the disease become eliminated in the community.

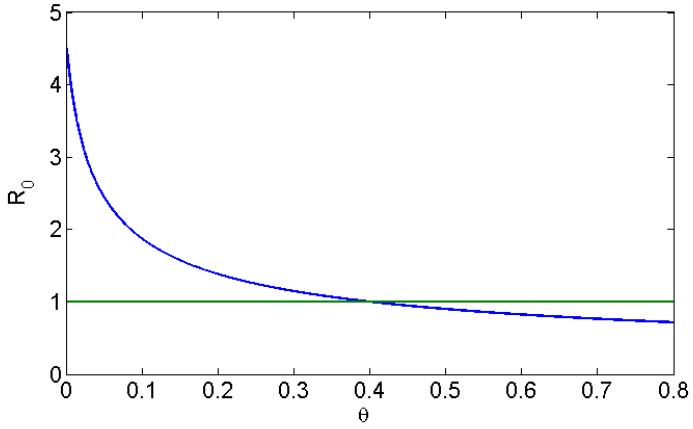

FIGURE 4. Effect of varying human awareness θ on R_0

Simulation results in Fig. 4, depicts the effects of varying human awareness rate θ on R_0. The results shows that an increase in human awareness rate (modeled by parameter θ) decreases the size of R_0. In particular, whenever $\theta > 0.4$, then $R_0 < 1$ which implies that it increases the human awareness rate by more than 40% the disease dies in the community.

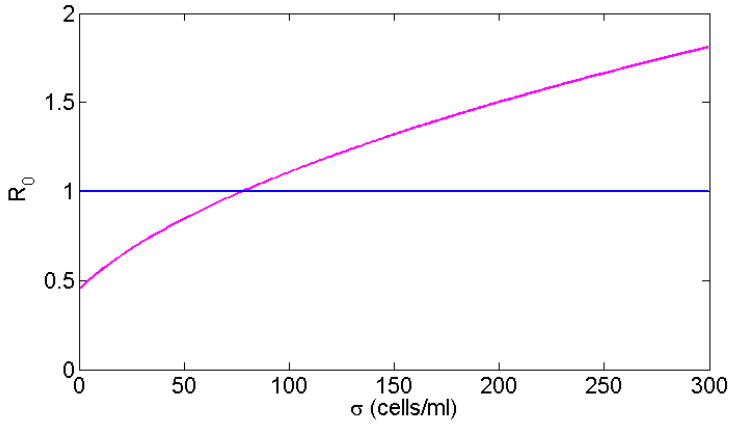

FIGURE 5. Effects of varying Shedding rate of vibrio bacteria σ on R_0

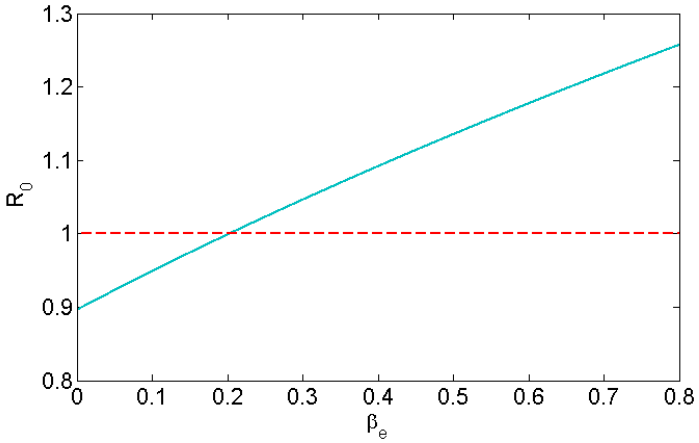

FIGURE 6. Effects of varying the rate of disease transmission between humans and environment β_e on R_0

Numerical results in Fig. 5, shows the effects of varying shedding rate of infected humans in the environment σ on R_0. From the results we observed that increasing the shedding rate of infected human in the environment (modeled by parameter σ) the disease persists in the community. In Fig. 6, shows the effect of varying the probability of disease transmission from environment to susceptible humans. One can note that increasing the risks of disease transmission from environment to susceptible humans, β_e the disease persists in the community.

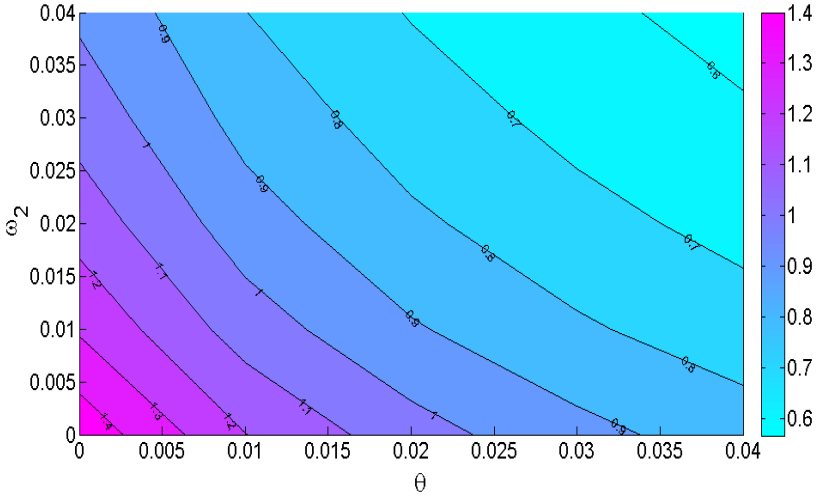

FIGURE 7. A contour plot of R_0 as the function of hygiene practices (modeled by the parameter ω_2) and health education campaigns (modeled by the parameter θ)

Figure (7) shows the contour plot of R_0 as function of hygiene practices and social mobilization on cleaning the environment ω_2 and education campaigns θ on reducing the spread of cholera disease in the community. From numerical simulation, it was noted that increasing the rate of hygiene practices and education campaigns θ, can lead to elimination of the disease in the population. This results demonstrate the effect of health education campaign and hygiene practice on reducing the spread of cholera disease in the population.

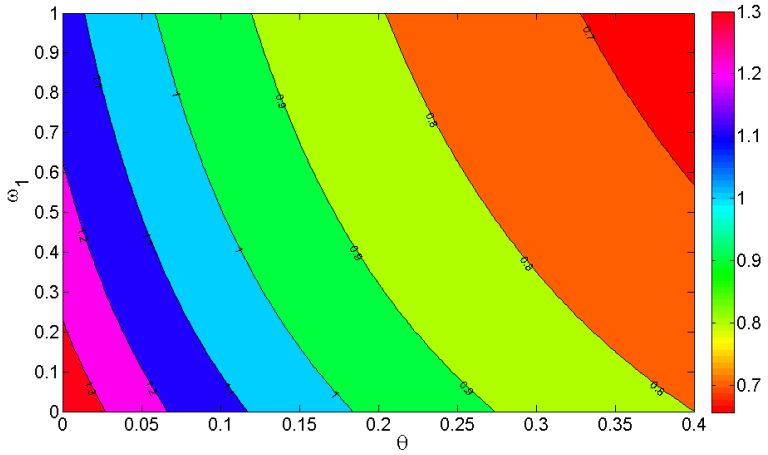

FIGURE 8. A contour plot of R_0 as the function of rate of treatment on infected human (modeled by the parameter ω_1) and health education campaign (modeled by the parameter θ)

Figure (8) depicts the contour plot of R_0 as a function of treatment on infected human ω_1, and health education campaign θ. The numerical results demonstrated that increasing the rate of treatment on infected humans ω_1 and use of health education campaigns θ reduce the magnitude of basic reproduction number R_0. In particular, one can note that the rate of health education campaign must be greater that 20% for the disease to be eliminated in the community.

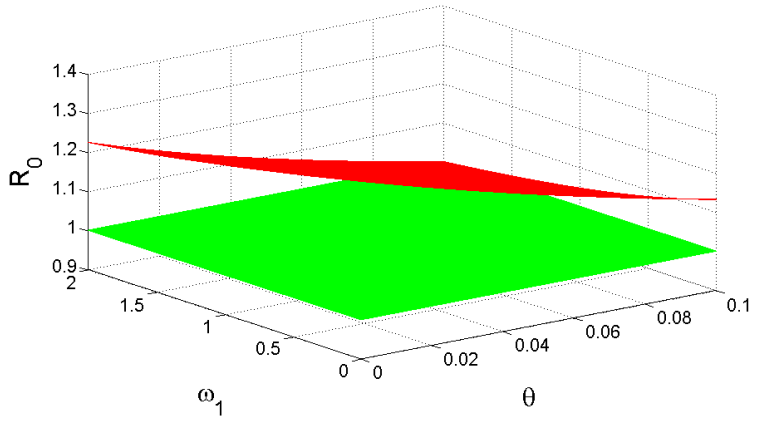

FIGURE 9. A mesh plot of the model system (1) to show the effect of treatment on infected humans (modeled by the parameter ω_1) and health education campaign (modeled by the parameter θ)

Figure (9) depicts the mesh plot of R_0 as a function of treatment on infected humans ω_1, and health education campaign θ on reducing the spread of cholera disease in the community. From numerical simulation, one can observe that both treatment on infected humans ω_1, and health education campaigns θ have the potential to reduce the magnitude of basic reproduction number R_0. The result demonstrate that increasing the aforementioned parameters minimize the spread of cholera disease in the community.

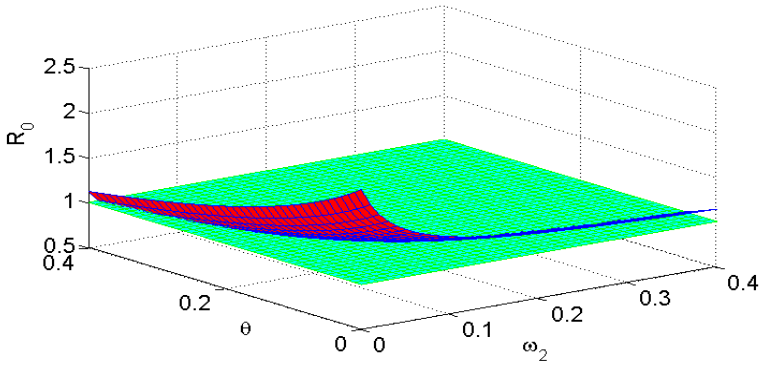

FIGURE 10. A mesh plot of the model system (1) to show the effect of hygiene practice (modeled by parameter ω_2), and health education campaign (modeled by the parameter θ)

4.3. Fitting the proposed model with cholera cases reported in Tanzania. In this section, we use the real data of cholera cases from Tanzania as reported in [29] to fit in the proposed model (1). The present data are yearly reported from 1998 to 2010 as presented in table (1). We utilized the Adam-Bashforth-Moulton scheme presented in (31) to numerically fit the real data in the model, and the commutative new infections predicted by the model (1) is obtained using the equation (35):

$$ {}_{b}^{c}D_{t}^{q}C(t) = \beta_h I(t)S(t) + \frac{\beta_e S(t)B(t)}{k+B(t)} \tag{35} $$

TABLE 3. Commutative of cholera cases in Tanzania from 1998 to 2010 as reported in [29]

Year	1998	1999	2000	2001	2002	2003	2004
Cases	296	12266	4637	2154	12403	12919	9639
Year	2005	2006	2007	2008	2009	2010	
Cases	3284	14297	2860	1619	6295	5566	

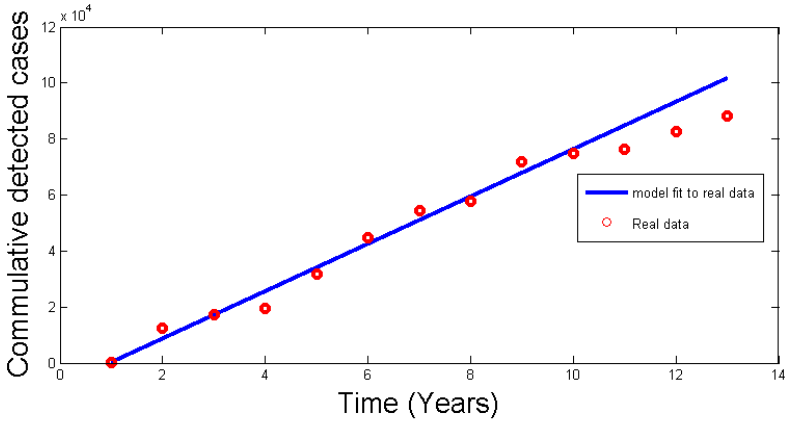

FIGURE 11. The model system (1) fitted to cholera cases in Tanzania at $q = 0.23$. The *red circles* indicate the real data and the *smooth line* denotes the model fit to the real data. We used the cholera cases as reported in [29]

Figure (11) denotes the commutative detected cholera cases in Tanzania. We used the cases reported in [29] to fit the model system (1) at the order of derivative $q = 0.23$. The results show that the model system (1) fit well on reported cholera cases in Tanzania.

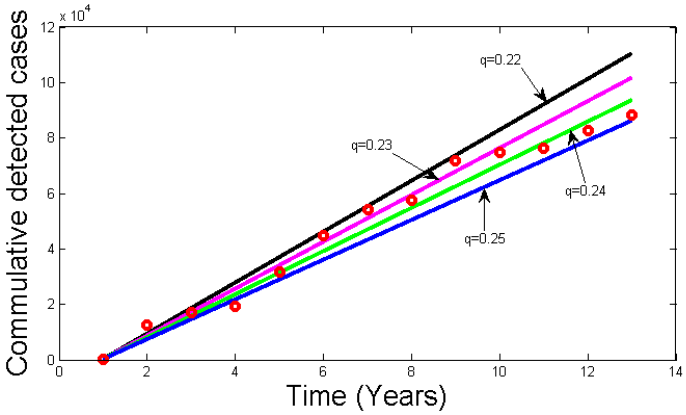

FIGURE 12. The model system (1) was fit to cholera cases in Tanzania at $q = 0.22$, $q = 0.23$, $q = 0.24$, and $q = 0.25$. The *red circles* indicate the real data and the *smooth line* indicates the model fit to the real data. We used the cholera cases as reported in [29].

Figure (12) shows the commutative detected cases of cholera cases in Tanzania at different fractional-order of derivatives. We used the cholera cases in Tanzania as reported in [29] to fit the model system (1) at $q = 0.22$, $q = 0.23$, $q = 0.24$, and $q = 0.25$. It was noted that at different values of memory species the model system (1) fits well with cholera cases reported in Tanzania.

4.4. Simulation of the model to support the analytical results. In this section, we simulated the model (1) at $q \in (0, 1]$ to support the analytical results. We first simulate the model at $R_0 < 1$, followed by simulation at $R_0 > 1$ and show the behavior of solution profiles in a long-range of interaction between humans, pathogens and environment.

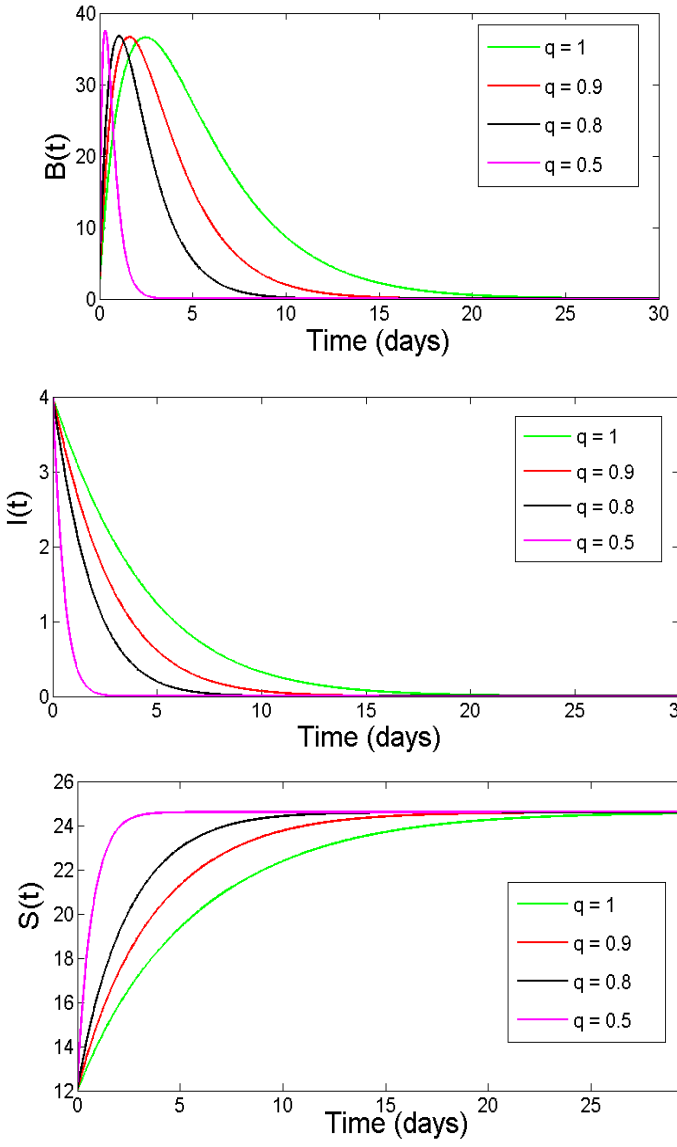

FIGURE 13. Simulation of the model system (1) to show the convergence of solution profiles at $R_0 < 1$

Figure (13) shows the simulation of model (1) to demonstrate the convergence of solution to the disease-free equilibrium point. We simulated the model at $R_0 \leq 0.1163$ with $\omega_1 = 0.01$, $\omega_2 = 0.6$, and $\theta = 0.18$. We observed that by varying the fractional order derivative q, the solution profile of the model converge to unique point which is equilibrium point. In particular, the disease can be eliminated in the population after 15 days of infections. Additionally, as the order of derivatives decrease from integer the solution of model attain its stability much faster compared to that close of integer order derivative.

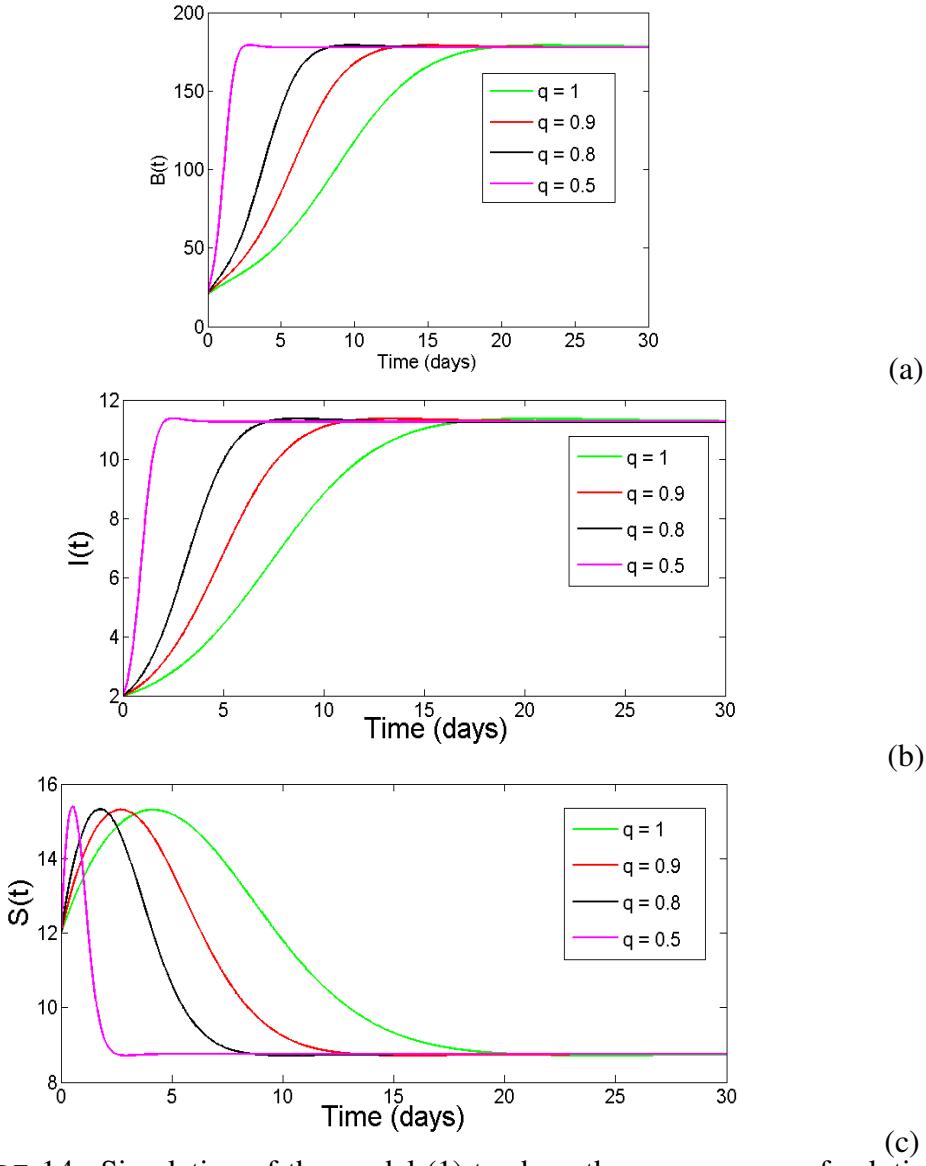

FIGURE 14. Simulation of the model (1) to show the convergence of solution profiles at $R_0 > 1$.

Figure (14) depicts the simulation of model (1) to show the convergence of solutions at the endemic equilibrium point. We simulated the model at $R_0 > 13.3332$ with $\omega_1 = 0.001$, $\omega_2 = 0.06$, and $\theta = 0.018$. We noted that, at different values of fractional order derivatives q, the solution profiles converge to the endemic equilibrium point. In particular we observed that after 20 days of infections the disease persists in the population.

5. CONCLUSION REMARKS

In this work, a fractional-order model for cholera disease transmission was proposed and studied. The model analysis was carried out and the results revealed that there exists global stability of disease-free and endemic equilibrium points whenever $R_0 \leq 1$ and $R_0 > 1$ respectively. We also performed the Sensitivity analysis of the model and the results showed that some parameters have a major influence on the spread of cholera disease in the community. From numerical simulations, We have used the Matlab programming to simulate the proposed model (1) at $R_0 < 1$ and $R_0 > 1$ to support the analytical results. We observed that for $R_0 < 1$, all solution profile of the model converge to the disease-free equilibrium point. In particular, after 15 days the disease dies in the population. Further more, we noted that as the order of derivatives decrease from integer the number of infections also decrease in the community.

Further more, we performed the sensitivity analysis of the model and we noted that some parameters have influence on spread of the disease in the community. In particular, increasing the shading rate of vibrio bacteria from infected humans in environment lead increase on the spread of disease in the population. Also, we used the real data of cholera cases in Tanzania as reported in [29] to fit in the proposed model. We noted that the formulated model fits well to the reported cholera cases in Tanzania. To minimize the spread of the disease in the population, we incorporated three control strategies in the proposed model namely; health education campaign, hygiene practice, and treatment of infected individuals. From the numerical simulations, we noted that, implementing human awareness by 40%, hygiene practices by 15% and treatment of infected humans by 20% can lead to elimination of the disease in the population. Finally, we simulated the model to support the analytical results at $R_0 < 1$ followed by simulations at $R_0 > 1$. The results showed that at different values of order of derivative, the solution profile of the model attains its stability at the equilibrium point which agree with analytical result on existence of global stability. In future, we will take and improve the formulated model by incorporating human movement and assess their effect on the dynamics of cholera disease in the population.

DATA AVAILABILITY

All data used in this paper included.

AUTHORS' CONTRIBUTIONS

All authors have equal contributions and they read and approved the final version of the paper.

CONFLICT OF INTERESTS

The authors declare that there is no conflict of interests.

REFERENCES

[1] J.P. La Salle, The stability of dynamical systems, Society for Industrial and Applied Mathematics, 1976. https://doi.org/10.1137/1.9781611970432.

[2] O. Diekmann, J.A.P. Heesterbeek, J.A.J. Metz, On the definition and the computation of the basic reproduction ratio R 0 in models for infectious diseases in heterogeneous populations, J. Math. Biol. 28 (1990), 365-382. https://doi.org/10.1007/BF00178324.

[3] C. Vargas-De-León, Volterra-type Lyapunov functions for fractional-order epidemic systems, Commun. Nonlinear Sci. Numer. Simul. 24 (2015), 75–85. https://doi.org/10.1016/j.cnsns.2014.12.013.

[4] M. Caputo, Linear models of dissipation whose Q is almost frequency independent–II, Geophys. J. Int. 13 (1967), 529–539. https://doi.org/10.1111/j.1365-246X.1967.tb02303.x.

[5] K. Diethelm, The analysis of fractional differential equations: an application-oriented exposition using differential operators of Caputo type, Springer-Verlag, Heidelberg, New York, 2010.

[6] P. van den Driessche, J. Watmough, Reproduction numbers and sub-threshold endemic equilibria for compartmental models of disease transmission, Math. Biosci. 180 (2002), 29-48. https://doi.org/10.1016/S0025-5564(02)00108-6.

[7] M. Helikumi, M. Kgosimore, D. Kuznetsov, S. Mushayabasa, Backward bifurcation and optimal control analysis of a trypanosoma brucei rhodesiense model, Mathematics. 7 (2019), 971. https://doi.org/10.3390/math7100971.

[8] L. Arriola, J. Hyman, Forward and adjoint sensitivity analysis with applications in dynamical systems, Lecture Notes in Linear Algebra and Optimization, (2005).

[9] J. Cui, Z. Wu, X. Zhou, Mathematical analysis of a cholera model with vaccination, J. Appl. Math. 2014 (2014), 324767. https://doi.org/10.1155/2014/324767.

[10] A. Mwasa, J.M. Tchuenche, Mathematical analysis of a cholera model with public health interventions, Biosystems. 105 (2011), 190–200. https://doi.org/10.1016/j.biosystems.2011.04.001.

[11] O.O. Okundalaye, W.A.M. Othman, A new optimal homotopy asymptotic method for fractional optimal control problems, Int. J. Differ. Equ. 2021 (2021), 6633130. https://doi.org/10.1155/2021/6633130.

[12] R.P. Sanches, C.P. Ferreira, R.A. Kraenkel, The role of immunity and seasonality in cholera epidemics, Bull. Math. Biol. 73 (2011), 2916–2931. https://doi.org/10.1007/s11538-011-9652-6.

[13] C.T. Codeço, Endemic and epidemic dynamics of cholera: the role of the aquatic reservoir. BMC Infect. Dis. 1 (2001), 1. https://doi.org/10.1186/1471-2334-1-1.

[14] B. Moses, Modeling the dynamics of cholera through controlling latrine waste in unofficial drainage system in Tanzania, University of Dar es Salaam, (2017).

[15] N. Kwasi-Do Ohene Opoku, C. Afriyie, The Role of Control Measures and the Environment in the Transmission Dynamics of Cholera, Abstr. Appl. Anal. 2020 (2020), 2485979. https://doi.org/10.1155/2020/2485979.

[16] T. Mashe, D. Domman, A. Tarupiwa, et al. Highly Resistant Cholera Outbreak Strain in Zimbabwe, N. Engl. J. Med. 383 (2020), 687–689. https://doi.org/10.1056/NEJMc2004773.

[17] F. Federspiel, M. Ali, The cholera outbreak in Yemen: lessons learned and way forward, BMC Public Health. 18 (2018), 1338. https://doi.org/10.1186/s12889-018-6227-6.

[18] G. Dinede, A. Abagero, T. Tolosa, Cholera outbreak in Addis Ababa, Ethiopia: A case-control study, PLoS ONE. 15 (2020), e0235440. https://doi.org/10.1371/journal.pone.0235440.

[19] G. George, J. Rotich, H. Kigen, et al. Notes from the field: Ongoing cholera outbreak–Kenya, 2014–2016, MMWR Morb. Mortal. Wkly. Rep. 65 (2016), 68–69. https://doi.org/10.15585/mmwr.mm6503a7.

[20] Y.M.G. Hounmanou, K. Mølbak, J. Kähler, R.H. Mdegela, J.E. Olsen, A. Dalsgaard, Cholera hotspots and surveillance constraints contributing to recurrent epidemics in Tanzania, BMC Res. Notes. 12 (2019), 664. https://doi.org/10.1186/s13104-019-4731-0.

[21] E.J. Nelson, J.B. Harris, J. Glenn Morris, S.B. Calderwood, A. Camilli, Cholera transmission: the host, pathogen and bacteriophage dynamic, Nat. Rev. Microbiol. 7 (2009), 693–702. https://doi.org/10.1038/nrmicro2204.

[22] J.P. Tian, S. Liao, J. Wang, Dynamical analysis and control strategies in modeling cholera. Preprint. (2010). https://web.nmsu.edu/~jtian/PB/2013-2.pdf.

[23] S.A. Fakai, M.O. Ibrahim, A.M. Siddiqui, A deterministic mathematical model on cholera dynamics and some control strategies, Int. J. Sci. Eng. Technol. 8 (2014), 1115-1118.

[24] B. Singer, Mathematical models of infectious diseases: Seeking new tools for planning and evaluating control programs, Popul. Develop. Rev. 10 (1984), 347-365.

[25] M.J. Ochoche, E.C. Madubueze, T.B. Akaabo, A mathematical model on the control of cholera: hygiene consciousness as a strategy, J. Math. Comput. Sci. 5 (2015), 172-187.

[26] Z. Mukandavire, S. Liao, J. Wang, H. Gaff, D.L. Smith, J.G. Morris, Estimating the reproductive numbers for the 2008–2009 cholera outbreaks in Zimbabwe, Proc. Natl. Acad. Sci. U.S.A. 108 (2011), 8767–8772. https://doi.org/10.1073/pnas.1019712108.

[27] R.L. Miller Neilan, E. Schaefer, H. Gaff, K.R. Fister, S. Lenhart, Modeling optimal intervention strategies for cholera, Bull. Math. Biol. 72 (2010), 2004–2018. https://doi.org/10.1007/s11538-010-9521-8.

[28] D.M. Hartley, J.G. Morris, D.L. Smith, Hyperinfectivity: A critical element in the ability of V. cholerae to cause epidemics? PLoS Med. 3 (2005), e7. https://doi.org/10.1371/journal.pmed.0030007.

[29] N. Ainea, A.X. Matofali, M. Mkwizu, Optimal control analysis of a cholera disease transmission model in Tanzania, Int. J. Innov. Res. Sci. Eng. Technol. 4 (2019), 865-872.

[30] A.A. Ayoade, M.O. Ibrahim, O.J. Peter, F.A. Oguntolu, A mathematical model on cholera dynamics with prevention and control, Covenant J. Phys. Life Sci. 6 (2018), 46-54.

[31] P. Panja, Optimal control analysis of a cholera epidemic model, Biophys. Rev. Lett. 14 (2019), 27-48. https://doi.org/10.1142/S1793048019500024.

[32] O.J. Peter, A.A. Ayoade, A.I. Abioye, A.A. Victor, C.E. Akpan, Sensitivity analysis of the parameters of a cholera model, J. Appl. Sci. Environ. Manage. 22 (2018), 477-481. https://doi.org/10.4314/jasem.v22i4.6.

[33] G.Q. Sun, J.H. Xie, S.H. Huang, Z. Jin, M.T. Li, L. Liu, Transmission dynamics of cholera: Mathematical modeling and control strategies, Commun. Nonlinear Sci. Numer. Simul. 45 (2017), 235–244. https://doi.org/10.1016/j.cnsns.2016.10.007.

[34] E.A. Bakare, S. Hoskova-Mayerova, Optimal control analysis of cholera dynamics in the presence of asymptotic transmission, Axioms. 10 (2021), 60. https://doi.org/10.3390/axioms10020060.

[35] A. Abebe, A mathematical model for transmission dynamics of cholera with control strategie, Thesis, Adama Science and Technology University, (2019).

[36] M. Hassouna, E.H. El Kinani, A. Ouhadan, Global existence and uniqueness of solution of Atangana–Baleanu Caputo fractional differential equation with nonlinear term and approximate solutions, Int. J. Differ. Equ. 2021 (2021), 5675789. https://doi.org/10.1155/2021/5675789.

[37] M. Altaf Khan, S. Ullah, M. Farooq, A new fractional model for tuberculosis with relapse via Atangana–Baleanu derivative, Chaos Solitons Fractals. 116 (2018), 227–238. https://doi.org/10.1016/j.chaos.2018.09.039.

[38] M. Helikumi, M. Kgosimore, D. Kuznetsov, S. Mushayabasa, Dynamical and optimal control analysis of a seasonal Trypanosoma brucei rhodesiense model, Math. Biosci. Eng. 17 (2020), 2530–2556. https://doi.org/10.3934/mbe.2020139.

[39] S.A.A. Shah, M.A. Khan, M. Farooq, S. Ullah, E.O. Alzahrani, A fractional order model for Hepatitis B virus with treatment via Atangana–Baleanu derivative, Physica A: Stat. Mech. Appl. 538 (2020), 122636. https://doi.org/10.1016/j.physa.2019.122636.

[40] K. Rajagopal, N. Hasanzadeh, F. Parastesh, I.I. Hamarash, S. Jafari, I. Hussain, A fractional-order model for the novel coronavirus (COVID-19) outbreak, Nonlinear Dyn. 101 (2020), 711–718. https://doi.org/10.1007/s11071-020-05757-6.

[41] I. Podlubny, Fractional differential equations: an introduction to fractional derivatives, fractional differential equations, to methods of their solution and some of their applications, Academic Press, San Diego, 1999.

[42] H. Delavari, D. Baleanu, J. Sadati, Stability analysis of Caputo fractional-order nonlinear systems revisited, Nonlinear Dyn. 67 (2012), 2433-2439. https://doi.org/10.1007/s11071-011-0157-5.

[43] M. Yavuz, E. Bonyah, New approaches to the fractional dynamics of schistosomiasis disease model, Physica A: Stat. Mech. Appl. 525 (2019), 373–393. https://doi.org/10.1016/j.physa.2019.03.069.

[44] B.S.T. Alkahtani, Atangana-Batogna numerical scheme applied on a linear and non-linear fractional differential equation, Eur. Phys. J. Plus. 133 (2018), 111. https://doi.org/10.1140/epjp/i2018-11961-8.

[45] A. Atangana, K.M. Owolabi, New numerical approach for fractional differential equations, Math. Model. Nat. Phenom. 13 (2018), 3. https://doi.org/10.1051/mmnp/2018010.

[46] M. Toufik, A. Atangana, New numerical approximation of fractional derivative with non-local and non-singular kernel: Application to chaotic models, Eur. Phys. J. Plus. 132 (2017), 444. https://doi.org/10.1140/epjp/i2017-11717-0.

[47] C.M.A. Pinto, J.A. Tenreiro Machado, Fractional model for malaria transmission under control strategies, Computers Math. Appl. 66 (2013), 908–916. https://doi.org/10.1016/j.camwa.2012.11.017.

[48] F.T. Akyildiz, F.S. Alshammari, Complex mathematical SIR model for spreading of COVID-19 virus with Mittag-Leffler kernel, Adv. Differ. Equ. 2021 (2021), 319. https://doi.org/10.1186/s13662-021-03470-1.

[49] S.O. Akindeinde, E. Okyere, A.O. Adewumi, R.S. Lebelo, O.O. Fabelurin, S.E. Moore, Caputo fractional-order SEIRP model for COVID-19 Pandemic, Alexandria Eng. J. 61 (2022), 829–845. https://doi.org/10.1016/j.aej.2021.04.097.

[50] A.S. Shaikh, K. Sooppy Nisar, Transmission dynamics of fractional order Typhoid fever model using Caputo–Fabrizio operator, Chaos Solitons Fractals. 128 (2019), 355–365. https://doi.org/10.1016/j.chaos.2019.08.012.

[51] N.H. Tuan, H. Mohammadi, S. Rezapour, A mathematical model for COVID-19 transmission by using the Caputo fractional derivative, Chaos Solitons Fractals. 140 (2020), 110107. https://doi.org/10.1016/j.chaos.2020.110107.

[52] S.T.M. Thabet, M.S. Abdo, K. Shah, T. Abdeljawad, Study of transmission dynamics of COVID-19 mathematical model under ABC fractional order derivative, Results Phys. 19 (2020), 103507. https://doi.org/10.1016/j.rinp.2020.103507.

[53] P.A. Naik, M. Yavuz, S. Qureshi, J. Zu, S. Townley, Modeling and analysis of COVID-19 epidemics with treatment in fractional derivatives using real data from Pakistan, Eur. Phys. J. Plus. 135 (2020), 795. https://doi.org/10.1140/epjp/s13360-020-00819-5.